Title

Discovery and Characterization of a Thioesterase-Specific Monoclonal Antibody That Recognizes the 6-Deoxyerythronolide B Synthase

Journal

Biochemistry, 57(43)

ISSN

0006-2960

Authors

Li, Xiuyuan
Sevillano, Natalia
La Greca, Florencia
et al.

Publication Date

2018-10-30

DOI

10.1021/acs.biochem.8b00886

Peer reviewed

HHS Public Access

Author manuscript

Biochemistry. Author manuscript; available in PMC 2019 October 30.

Published in final edited form as:

Biochemistry. 2018 October 30; 57(43): 6201–6208. doi:10.1021/acs.biochem.8b00886.

Discovery and Characterization of a Thioesterase-Specific Monoclonal Antibody That Recognizes the 6-Deoxyerythronolide B Synthase

Xiuyuan Li[†], **Natalia Sevillano**[⊥], **Florencia La Greca**[⊥], **Jake Hsu**[‡], **Irimpan I. Mathews**[#], **Tsutomu Matsui**[⊥], **Charles S. Craik**[⊥], and **Chaitan Khosla**[*,†,‡,§,∥]

[†]Department of Chemistry, Stanford University, Stanford, California 94305, United States

[‡]Department of Biochemistry, Stanford University, Stanford, California 94305, United States

[§]Department of Chemical Engineering, Stanford University, Stanford, California 94305, United States

[∥]Stanford ChEM-H, Stanford University, Stanford, California 94305, United States

[⊥]Department of Pharmaceutical Chemistry, University of California San Francisco, San Francisco, California 94158, United States

[#]Stanford Synchrotron Radiation Lightsource, SLAC National Accelerator Laboratory, Stanford University, Menlo Park, California 94025, United States

Abstract

Assembly line polyketide synthases (PKSs) are large multimodular enzymes responsible for the biosynthesis of diverse antibiotics in bacteria. Structural and mechanistic analysis of these megasynthases can benefit from the discovery of reagents that recognize individual domains or linkers in a site-specific manner. Monoclonal antibodies not only have proven themselves as premier tools in analogous applications but also have the added benefit of constraining the conformational flexibility of their targets in unpredictable but often useful ways. Here we have exploited a library based on the naïve human antibody repertoire to discover a F_{ab} (3A6) that recognizes the terminal thioesterase (TE) domain of the 6-deoxyerythronolide B synthase with high specificity. Biochemical assays were used to verify that 3A6 binding does not inhibit enzyme turnover. The co-crystal structure of the TE–3A6 complex was determined at 2.45 Å resolution, resulting in atomic characterization of this protein–protein recognition mechanism. F_{ab} binding had minimal effects on the structural integrity of the TE. In turn, these insights were used to interrogate via small-angle X-ray scattering the solution-phase conformation of 3A6 complexed to a catalytically competent PKS module and bimodule. Altogether, we have developed a high-affinity monoclonal antibody tool that recognizes the TE domain of the 6-deoxyerythronolide B synthase while maintaining its native function.

Graphical Abstract

[*]**Corresponding Author** khosla@stanford.edu.

Notes

The authors declare no competing financial interest.

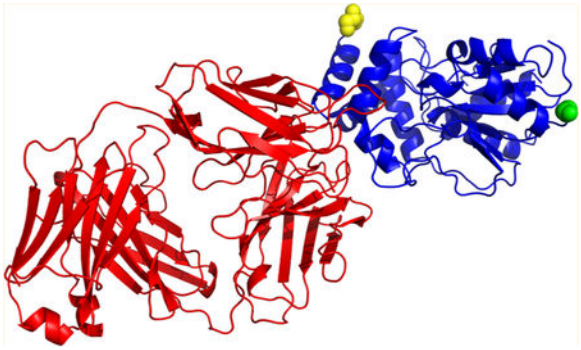

Assembly line polyketide synthases (PKSs) are multifunctional enzymes that catalyze the biosynthesis of many natural products by channeling reactive intermediates through a unique sequence of enzymatic active sites.[1,2] For example, the 6-deoxyerythronolide B synthase [DEBS (Figure 1A)] synthesizes the macrocyclic core of the antibiotic erythromycin via sequential actions of 22 enzymatic domains.[3,4] These domains are organized into six chain elongation "modules" flanked by a loading didomain that promotes chain initiation and a thioesterase (TE) domain that catalyzes chain release.[5] Thus, the architecture of DEBS somehow establishes a unique pathway for channeling the growing polyketide chain through a sequence of active sites, as it is elaborated into 6-deoxyerythronolide B. Throughout this catalytic cycle, the chain remains covalently bound to individual acyl carrier protein (ACP) and ketosynthase (KS) domains via thioester linkages.[6] One can reasonably assume that a subset of the ~30 domains of DEBS must exhibit considerable conformational flexibility in the context of this remarkable catalytic cycle, although such flexibility has never been visualized, nor is its mechanistic basis well understood.

To facilitate analysis of DEBS with an eye toward the challenges described above, we have sought to develop tools for enhanced visualization of this assembly line (or parts thereof) on varying length and time scales. Monoclonal antibodies are powerful reagents for such applications.[7–10] In particular, F_{ab} (fragment antigen-binding) antibodies are known to form rigid complexes with their antigens.[9] Using a phage display library based on the naïve human antibody repertoire, we recently reported the discovery of a F_{ab} (1B2) that trapped a target PKS module in a previously characterized conformation.[11,12] Isolation of 1B2 proved to be invaluable in addressing the catalytic relevance of this module conformation. Building on that successful example, we also sought an antibody against the TE domain of DEBS. Here we describe the results of these efforts.

EXPERIMENTAL PROCEDURES

Cloning, Expression, and Purification of DEBS Proteins.

DEBS proteins or derivatives thereof were expressed in *Escherichia coli* and purified according to previously described protocols.[6,11–14]

Fab Selection and Verification.

F_{ab} selection was performed using a fully human naïve F_{ab} phage display library.[15] Library panning was performed according to previously described protocols.[1,16] DEBS module 3+TE was first lightly biotinylated with NHS-PEG_{12}-biotin reagent (EZ-Link). The extent of biotinylation was quantified with a HABA kit (Pierce) and controlled to be slightly less than one biotin per protein to minimize disruption of enzyme function. The target was then immobilized on streptavidin-coated magnetic beads and panned against the library for three rounds. The resulting clones were grown, and culture supernatants were screened for binding with an enzyme-linked immunosorbent assay (ELISA). Positive clones were used for further analysis.

Expression and Periplasmic Extraction of F_{ab}.

F_{ab} was produced following a previously described protocol.[11,17] The 3A6-encoding phagemid was introduced via transformation into *E. coli* BL21(DE3). Cells were grown in 2×YT with carbenicillin (100 μg/mL) and 0.1% (w/v) glucose at 37 °C and 250 rpm until the OD_{600} reached 0.6–0.8. The cultures were then cooled to 20 °C, induced with the addition of 1 mM isopropyl β-D-1-thiogalactopyranoside, and shaken for an additional 12–14 h at 180 rpm. The bacteria were pelleted by centrifugation at 6300g for 10 min. Periplasmic extraction was performed by first resuspending cells in TES buffer [0.2 M Tris (pH 8.0), 0.5 mM ethylenediaminetetraacetic acid (EDTA), and 0.5 M sucrose; 20 mL/L of pellet] for 2 h at 4 °C under stirring. Then 20 mL of deionized water was added. The solution was stirred at 4 °C for a further 1 h, and the insoluble fraction was pelleted at 25000g. The supernatant, supplemented with 2 mM $MgCl_2$ and 10 mM imidazole, was then incubated overnight with 2 mL of Ni-NTA resin. The Ni-NTA resin was then washed with 5 column volumes (CV) of wash buffer I [250 mM NaCl and 50 mM Tris (pH 8.0)] followed by 5 CV of wash buffer II [20 mM imidazole, 500 mM NaCl, and 50 mM Tris (pH 8.0)], and the F_{ab} was eluted with 3 CV of elution buffer [500 mM imidazole, 100 mM NaCl, and 50 mM Tris (pH 8.0)]. The pooled eluent was concentrated to 500 μL and polished on a Superdex 200 10/30 column (GE Healthcare) in 10 mM HEPES and 250 mM NaCl (pH 8.0) (SEC buffer). The F_{ab} concentration was quantified by the BCA assay (Pierce).

Enzymatic Assays.

Assays for measuring the steady-state rate of polyketide synthesis were performed as previously reported.[6] Briefly, 2 μM DEBS proteins (LDD, M1, M2, and M3+TE) with or without 2.5 μM 3A6 were added to 400 mM sodium phosphate (pH 7.2) containing 5 mM TCEP, 10 mM $MgCl_2$, 2 mM coenzyme A, and 2.5 mM ATP. Enzymes MatB (malonyl-CoA synthetase, 2 μM) and methylmalonyl-CoA epimerase (4 μM) were included to convert methylmalonic acid into racemic methylmalonyl-CoA.[18] The reaction rate was monitored at 340 nm using a Lambda-25 ultraviolet–visible spectrophotometer (PerkinElmer).

Crystallization.

The F_{ab}–TE complex was produced in a manner similar to a previously reported procedure.[11] 3A6 and TE were mixed in a 1:1 ratio for 60 min at 4 °C, followed by purification using a Superdex 200 10/300 size exclusion chromatography (SEC) column (GE Healthcare) pre-

equilibrated with SEC buffer. Fractions corresponding to the complex were pooled and concentrated to 4.6 mg/mL. Crystals (space group H_{32}) were obtained by combining 0.15 μL of protein with 0.15 μL of screen [200 mM Na_2HPO_4, 20% (w/v) PEG 3350, and 15% (w/v) ethylene glycol] at 22 °C. Crystals were grown for 5 months and harvested by direct immersion in liquid N_2 without extra cryoprotectant. Data were collected on BL12-2 at the Stanford Synchrotron Radiation Lightsource (SSRL) at 100 K and processed with XDS.[19]

The structure of the F_{ab}–TE complex was determined by MOLREP.[20] After a number of unsuccessful attempts, the structure was determined by first fixing the TE domain [Protein Data Bank (PDB) entry 1MN6[21]] and performing a heteromultimer search by simultaneously searching for the N-terminus [residues 1–112 (chain A) and 1–130 (chain B)] and C-terminus [residues 115–217 (chain A) and 135–230 (chain B)] in the anti-CMV F_{ab} fragment (PDB entry 4LRI[22]). A rigid-body refinement at 3.0 Å using the resulting complex gave an R factor of 43%. The resulting structure went through model building cycles involving ARP/Warp,[23] Buccaneer,[24] and a number of manual model building cycles using COOT.[25] The later stages of refinement were carried out using PHENIX.[26] Water molecules were located by manual inspection of the $2F_o - F_c$ and $F_o - F_c$ electron density maps. The final refined model converged with R_{work} and R_{free} values of 17.5 and 23.5%, respectively. Coordinates were analyzed for all-atom contacts and correct geometry using MolProbity,[27] and the final coordinates were deposited in the Protein Data Bank as entry 6MLK.

Tandem Size Exclusion Chromatography and Small-Angle X-ray Scattering (SEC–SAXS).

SEC–SAXS analysis was performed on Bio-SAXS beamline BL4-2 at SSRL following a previous protocol with slight modification.[11,12] The experimental setup and structural parameters are summarized in Table 2.

For the M3TE–3A6 and DEBS3–3A6 complexes, the F_{ab} and the PKS homodimer were mixed at room temperature for 60 min in a 1.2:1 stoichiometry and then passed through a Superose 6 Increase 3.2/300 column (GE Healthcare) equilibrated with 200 mM sodium phosphate (pH 7.6) at a rate of 0.04 mL/min. Importantly, all SEC–SAXS experiments were performed in the buffer defined above, because maximum PKS activity critically depends on the presence of such a high phosphate concentration. In-line SAXS analysis was performed as the eluted complex passed into the detection capillary.

The quality of the data was carefully assessed, and the theoretical scattering curves were computed from alternative structural models using CRYSOL.[28] In turn, these scattering curves were compared to experimental data (Figures 7 and 8).

RESULTS

Discovery of an Antibody against the TE Domain of DEBS.

Module 3+TE is a 372 kDa homodimeric protein comprised of the complete module 3 of DEBS fused to the terminal TE domain of this assembly line PKS (Figure 1B).[6] This protein was purified to homogeneity, lightly biotinylated (approximately one biotin substituent per monomer), immobilized on streptavidin beads, and used to select F_{ab} from a large phage

display library of 3.7×10^{10} F_{ab} fragments from the naive human antibody repertoire, as described previously.[14] The overall process yielded multiple, high-affinity clones against the target protein, one of which was shown to selectively bind to the stand-alone TE protein. This F_{ab} was designated 3A6, and its identity was established by DNA sequencing.

Binding Affinity Measurement.

Quantitative ELISA analysis of 3A6 against module 3+TE [M3+TE (Figure 2A)] and the stand-alone TE domain (Figure 2B) demonstrated that the antibody bound to both proteins with a comparably high affinity (K_D values of 42 ± 12 nM for M3+TE and 13 ± 2 nM for the TE alone). The affinity of the F_{ab} for the stand-alone TE was further verified by biolayer interferometry (FortBio Octet RED384) (Figure 2C; $K_D = 16 \pm 0.1$ nM, $k_{on} = 0.3\ \mu M^{-1}\ s^{-1}$, $k_{off} = 4.8 \times 10^{-3}\ s^{-1}$). SEC analysis further verified the stability and homogeneity of the 3A6–TE complex (Figure 3A), while sodium dodecyl sulfate–polyacrylamide gel electrophoresis (SDS–PAGE) of the SEC peak fraction confirmed stoichiometric co-elution of both 3A6 and TE (Figure 3B). The molecular weight (MW) of the complex was estimated to be 240 kDa via SEC analysis, suggesting that 3A6-TE likely exists as a dimer in solution (calculated MW = 178 kDa).

Effect of 3A6 Binding on the Catalytic Activity of the TE Domain.

The structurally characterized TE domain of DEBS receives its acyl chain substrate from the ACP domain of module 6 and catalyzes polyketide chain release via concomitant macrolactonization.[3,21,30] To evaluate the effects, if any, of 3A6 binding on these catalytic properties, the antibody was added to a previously developed steady-state turnover assay of the trimodular truncated derivative of DEBS (Figure 1B).[6] Here, TE is indispensable for PKS turnover, because in the absence of this domain, product release occurs at an insignificantly low rate. At 2 μM concentrations of each of the four homodimeric PKS proteins in this assay, addition of excess 3A6 (2.5 μM) had no measurable effect on steady-state turnover kinetics (Figure 4). Thus, we can conclude that 3A6 binds to the TE domain in a manner that does not adversely affect the biosynthesis of tetraketide lactone by the trimodular construct.

X-ray Crystallographic Analysis of the 3A6–TE Complex.

Co-crystals of the 3A6–TE complex were grown from SEC-purified protein, as described above. Crystals belonged to hexagonal space group H_{32} and diffracted to 2.45 Å resolution (Table 1). The structure was refined to R_{work} and R_{free} values of 17.5 and 23.5%, respectively. The atypically high B factor was likely due to a less stable crystal, in part because of radiation decay and also a reduced level of crystal packing.

As seen in Figure 5A, each asymmetric unit contained one copy each of the F_{ab} and the TE. Antibody 3A6 was bound principally through extensive hydrogen bonding to a structured region on the TE surface (Figure 5B) that is distant from the previously reported tunnel through which the substrate and product are thought to enter and exit, respectively, the active site.[21,29,30] Variable regions from both the heavy chain and light chain fragments contributed to interaction with TE (Figure 5B,C). Its binding to the TE appeared to represent an example of lock-and-key recognition, as no significant rearrangements were observed in the TE

backbone as a result of 3A6 binding (Figure 6A; root-mean-square deviation of 0.359 Å). In particular, the catalytic triad (Ser142-Asp169-His259) of the TE was maintained in its native geometry in the F_{ab}-bound structure (Figure 6B,C). Because the native TE is homodimeric in solution,[21,29,30] the two protomers were related by 2-fold rotational symmetry. The dimeric architecture was visualized through symmetry expansion and found to be unperturbed by binding to 3A6 (Figure 5D). In the dimeric complex, the two copies of F_{ab} were oriented at opposite ends of the TE homodimer and had no steric interaction with each other.

Solution-Phase SEC–SAXS Analysis of Binding of 3A6 to Catalytically Competent Module 3+TE and DEBS3.

To directly correlate the findings described above from solution-phase (Figures 2–4) and crystallographic (Figures 5 and 6) analyses, we subjected different antibody–PKS complexes to SEC–SAXS analyses under conditions affording high enzyme activity, using protocols entirely analogous to those detailed previously.[11,12] The SAXS data from each SEC peak fraction were compared to theoretical scattering curves generated by CRYSOL based on rigid-body docking of 3A6 to previously generated models of M3+TE (Figure 7) and the bimodular DEBS3 (Figure 8). In each case, the experimental data showed good correlation with the theoretically predicted scattering curves. A comparison of the log(*I*) versus q data for M3+TE with and without bound 3A6 is shown in panels B and E of Figure 7, respectively (χ^2 = 0.274 and χ^2 = 0.310, respectively); the corresponding Kratky plots are shown in panels C and F of Figure 7, respectively. The 3A6–DEBS3 complex was also analyzed via SEC–SAXS (Figure 8); again, a good correlation was observed between experimental and simulated data (χ^2 = 0.477). The overall statistics from SAXS analysis of both constructs are summarized in Table 2. Together, these results verified that antibody binding did not significantly alter the overall architecture of homodimeric PKS proteins harboring the DEBS TE domain.

DISCUSSION

Assembly line polyketide synthases are remarkably complex multienzyme systems in which the substrate that initiates polyketide chain growth is unidirectionally channeled across many active sites, thereby undergoing a tightly regulated sequence of chemical reactions. The exact mechanism of how this biosynthetic feat is synchronized over such a long distance presents a major fundamental challenge in enzymology. From a structural biological standpoint, one might expect a PKS assembly line to be inherently dynamic, thereby rendering it as a challenging target for analysis at high resolution. Dissection of the functional and structural details of assembly line PKSs warrants expansion of the current toolbox for studying these systems.

Recombinant antibodies have been particularly useful tools for structural analysis of complex protein systems.[7–10] We have therefore sought to discover, characterize, and deploy antibodies to target specific regions of DEBS, a prototypical assembly line PKS. Using a fully naïve human-derived library displayed on phage, we discovered a monoclonal F_{ab}, 3A6, which is specific for the terminal thioesterase of DEBS with near nanomolar affinity.

3A6 was shown to be a functionally neutral antibody with no detectable effect on enzymatic turnover or protein conformation, as demonstrated by a series of biophysical experiments and crystallographic analyses. Furthermore, SEC–SAXS analysis verified the lack of structural perturbation on homodimeric unimodular and bimodular PKSs in the solution phase. Thus, such an inert F_{ab} could be potentially developed into a tool for dynamic spectroscopic analysis or as a structural fiducial marker in electron microscopy.[31] Together with 1B2,[11] we have put forth two valuable and orthogonal F_{ab}s for structural and enzymological studies of DEBS. This discovery strategy is readily applicable to other complex multidomain enzyme systems.

ACKNOWLEDGMENTS

X-ray analysis was performed on beamline 12-2, and SEC–SAXS analysis was performed on beamline 4-2 at the Stanford Synchrotron Radiation Lightsource (SSRL), SLAC National Accelerator Laboratory. Use of the SSRL, SLAC National Accelerator Laboratory, is supported by the U.S. Department of Energy (DOE), Office of Science, Office of Basic Energy Sciences, under Contract DE-AC02-76SF00515. The SSRL Structural Molecular Biology Program is supported by the DOE Office of Biological and Environmental Research and by the National Institutes of Health, National Institute of General Medical Sciences (including Grant P41GM103393).

Funding

This research was supported by grants from the National Institutes of Health (GM087934 to C.K. and P41CA196276 and GM104659 to C.S.C.).

REFERENCES

(1). Walsh CT (2004) Polyketide and nonribosomal peptide antibiotics: modularity and versatility. Science 303, 1805. [PubMed: 15031493]

(2). Khosla C, Tang Y, Chen AY, Schnarr NA, and Cane DE (2007) Structure and mechanism of the 6-deoxyerythronolide B synthase. Annu. Rev. Biochem 76, 195. [PubMed: 17328673]

(3). Cortes J, Haydock SF, Roberts GA, Bevitt DJ, and Leadlay PF (1990) An unusually large multifunctional polypeptide in the erythromycin-producing polyketide synthase of Saccharopolyspora erythraea. Nature 348, 176. [PubMed: 2234082]

(4). Donadio S, Staver MJ, McAlpine JB, Swanson SJ, and Katz L (1991) Modular organization of genes required for complex polyketide biosynthesis. Science 252, 675. [PubMed: 2024119]

(5). Horsman ME, Hari TPA, and Boddy CN (2016) Polyketide synthase and non-ribosomal peptide synthetase thioesterase selectivity: logic gate or a victim of fate? Nat. Prod. Rep 33, 183. [PubMed: 25642666]

(6). Lowry B, Robbins T, Weng CH, O'Brien RV, Cane DE, and Khosla C (2013) In vitro reconstitution and analysis of the 6-deoxyerythronolide B synthase. J. Am. Chem. Soc. 135, 16809. [PubMed: 24161212]

(7). Malia TJ, Obmolova G, Luo J, Teplyakov A, Sweet R, and Gilliland GL (2011) Crystallization of a challenging antigen-antibody complex: TLR3 ECD with three noncompeting Fabs. Acta Crystallogr., Sect. F: Struct. Biol. Cryst. Commun 67, 1290.

(8). Zhou Y, Morais-Cabral JH, Kaufman A, and MacKinnon R (2001) Chemistry of ion coordination and hydration revealed by a K^+channel–Fab complex at 2.0 Å resolution. Nature 414, 43. [PubMed: 11689936]

(9). Uysal S, Vasquez V, Tereshko V, Esaki K, Fellouse FA, Sidhu SS, Koide S, Perozo E, and Kossiakoff A (2009) Crystal structure of full-length KcsA in its closed conformation. Proc. Natl. Acad. Sci. U. S. A 106, 6644. [PubMed: 19346472]

(10). Farady CJ, Egea PF, Schneider EL, Darragh MR, and Craik CS (2008) Structure of an Fab-protease complex reveals a highly specific non-canonical mechanism of inhibition. J. Mol. Biol 380, 351. [PubMed: 18514224]

(11). Li X, Sevillano N, La Greca F, Deis L, Liu YC, Deller MC, Mathews II, Matsui T, Cane DE, Craik CS, and Khosla C (2018) Structure-function analysis of the extended conformation of a polyketide synthase module. J. Am. Chem. Soc 140, 6518. [PubMed: 29762030]

(12). Edwards AL, Matsui T, Weiss TM, and Khosla C (2014) Architectures of whole-module and bimodular proteins from the 6-deoxyerythronolide B synthase. J. Mol. Biol 426, 2229. [PubMed: 24704088]

(13). Wu N, Cane DE, and Khosla C (2002) Quantitative analysis of the relative contributions of donor acyl carrier proteins, acceptor ketosynthases, and linker regions to intermodular transfer of intermediates in hybrid polyketide synthases. Biochemistry 41, 5056. [PubMed: 11939803]

(14). Chen AY, Schnarr NA, Kim CY, Cane DE, and Khosla C (2006) Extender unit and acyl carrier protein specificity of ketosynthase domains of the 6-deoxyerythronolide B synthase. J. Am. Chem. Soc 128, 3067. [PubMed: 16506788]

(15). Duriseti S, Goetz DH, Hostetter DR, LeBeau AM, Wei Y, and Craik CS (2010) Antagonistic anti-urokinase plasminogen activator receptor (uPAR) antibodies significantly inhibit uPAR-mediated cellular signaling and migration. J. Biol. Chem 285, 26878. [PubMed: 20501655]

(16). Kim J, Stroud RM, and Craik CS (2011) Rapid identification of recombinant Fabs that bind to membrane proteins. Methods 55, 303. [PubMed: 21958987]

(17). Kim J, Wu S, Tomasiak TM, Mergel C, Winter MB, Stiller SB, Robles-Colmanares Y, Stroud RM, Tampe R, Craik CS, and Cheng Y (2015) Subnanometre-resolution electron cryomicroscopy structure of a heterodimeric ABC exporter. Nature 517, 396. [PubMed: 25363761]

(18). Hughes AJ, and Keatinge-Clay AT (2011) Enzymatic extender unit generation for in vitro polyketide synthase reactions: structural and functional showcasing of Streptomyces coelicolor MatB. Chem. Biol 18, 165. [PubMed: 21338915]

(19). Kabsch W (2010) XDS. Acta Crystallogr., Sect. D: Biol. Crystallogr 66, 125. [PubMed: 20124692]

(20). Vagin A, and Teplyakov A (1997) *MOLREP*: an automated program for molecular replacement. J. Appl Crystallogr 30, 1022.

(21). Tsai SC, Lu H, Cane DE, Khosla C, and Stroud RM (2002) Insights into channel architecture and substrate specificity from crystal structures of two macrocycle-forming thioesterases of modular polyketide synthases. Biochemistry 41, 12598. [PubMed: 12379102]

(22). Fouts AE, Comps-Agrar L, Stengel KF, Ellerman D, Schoeffler AJ, Warming S, Eaton DL, and Feierbach B (2014) Mechanism for neutralizing activity by the anti-CMV gH/gL monoclonal antibody MSL-109. Proc. Natl. Acad. Sci. U. S. A 111, 8209. [PubMed: 24843144]

(23). Joosten K, Cohen SX, Emsley P, Mooij W, Lamzin VS, and Perrakis A (2008) A knowledge-driven approach for crystallographic protein model completion. Acta Crystallogr., Sect. D: Biol. Crystallogr 64, 416. [PubMed: 18391408]

(24). Cowtan K (2006) The Buccaneer software for automated model building. 1. Tracing protein chains. Acta Crystallogr., Sect. D: Biol. Crystallogr 62, 1002. [PubMed: 16929101]

(25). Emsley P, Lohkamp B, Scott W, and Cowtan K (2010) Features and development of Coot. Acta Crystallogr., Sect. D: Biol. Crystallogr 66, 486. [PubMed: 20383002]

(26). Adams PD, Afonine PV, Bunkoczi G, Chen VB, Davis IW, Echols N, Headd JJ, Hung LW, Kapral GJ, Grosse-Kunstleve RW, McCoy AJ, Moriarty NW, Oeffner R, Read RJ, Richardson DC, Richardson JS, Terwilliger TC, and Zwart PH (2010) *PHENIX*: a comprehensive Python-based system for macromolecular structure solution. Acta Crystallogr., Sect. D: Biol. Crystallogr 66, 213. [PubMed: 20124702]

(27). Chen VB, Arendall WB, III, Headd JJ, Keedy DA, Immormino RM, Kapral GJ, Murray LW, Richardson JS, and Richardson DC (2010) MolProbity: all-atom structure validation for macromolecular crystallography. Acta Crystallogr., Sect. D: Biol. Crystallogr 66, 12. [PubMed: 20057044]

(28). Svergun D, Barberato C, and Koch MHJ (1995) CRYSOL - a program to evaluate X-ray solution scattering of biological macromolecules from atomic coordinates. J. Appl. Crystallogr 28, 768.

(29). Tsai SC, Miercke LJ, Krucinski J, Gokhale R, Chen JC, Foster PG, Cane DE, Khosla C, and Stroud RM (2001) Crystal structure of the macrocycle-forming thioesterase domain of the

erythromycin polyketide synthase: versatility from a unique substrate channel. Proc. Natl. Acad. Sci. U. S. A 98, 14808. [PubMed: 11752428]

(30). Argyropoulos P, Bergeret F, Pardin C, Reimer JM, Pinto A, Boddy CN, and Schmeing TM (2016) Towards a characterization of the structural determinants of specificity in the macrocyclizing thioesterase for deoxyerythronolide B biosynthesis. Biochim. Biophys. Acta, Gen. Subj 1860, 486.

(31). Wu S, Avila-Sakar A, Kim J, Booth DS, Greenberg CH, Rossi A, Liao M, Li X, Alian A, Griner SL, Juge N, Yu Y, Mergel CM, Chaparro-Riggers J, Strop P, Tampe R, Edwards RH, Stroud RM, Craik CS, and Cheng Y (2012) Fabs enable single particle cryoEM studies of small proteins. Structure 20, 582. [PubMed: 22483106]

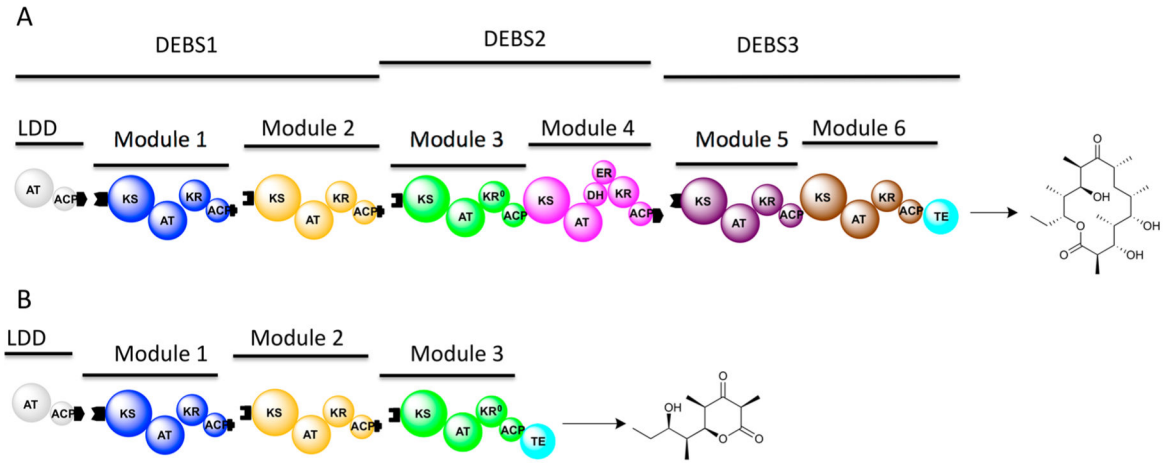

Figure 1.

(A) Synthesis of 6-deoxyerythronolide B by DEBS. Abbreviations: ACP, acyl carrier protein; AT, acyltransferase; DH, dehydratase; KR, ketoreductase; KR^0, inactive ketoreductase; KS, ketosynthase. Whereas the loading didomain (LDD) and the first two modules of DEBS occur within a single protein (DEBS1) in nature, our in vitro reconstituted system is derived from expressing and purifying the LDD and the two modules as separate proteins.[6] (B) The truncated trimodular derivative of DEBS exhibits all the properties of the first three modules of this assembly line PKS. Fusion of the thioesterase (TE) domain to module 3 results in the chimeric M3+TE protein and facilitates turnover of this truncated PKS.[6]

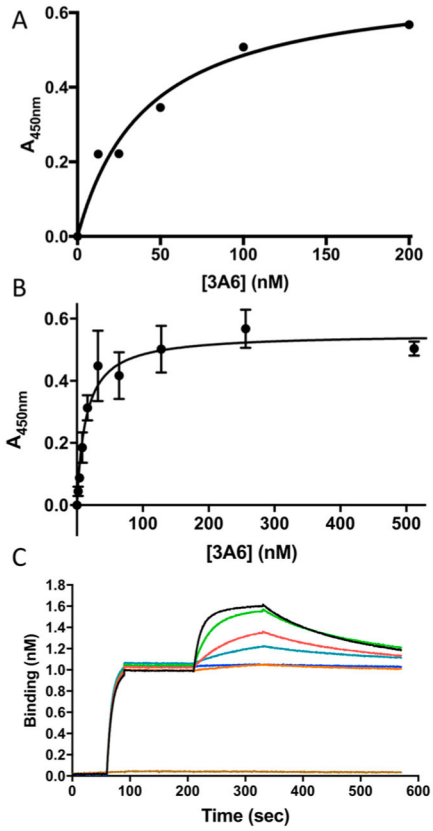

Figure 2.

Affinity of purified antibody 3A6 for its target proteins. (A) ELISA binding assay against immobilized M3+TE of DEBS. The measured affinity of 3A6 for M3+TE is 42 ± 12 nM. (B) Binding assay against the stand-alone TE domain. The measured affinity of 3A6 for the TE is 13 ± 2 nM. (C) Association and dissociation of 3A6 (black, 300 nM; green, 100 nM; red, 33 nM; cyan, 11 nM; orange, 3.7 nM; blue, 1.2 nM; brown, background without TE) with biotinylated stand-alone TE was monitored on an Octet RED96 instrument. The measured k_{on} = 0.3 μM^{-1} s^{-1}, k_{off} = 4.8 × 10^{-3} s^{-1}, and K_D = 16 ± 0.1 nM.

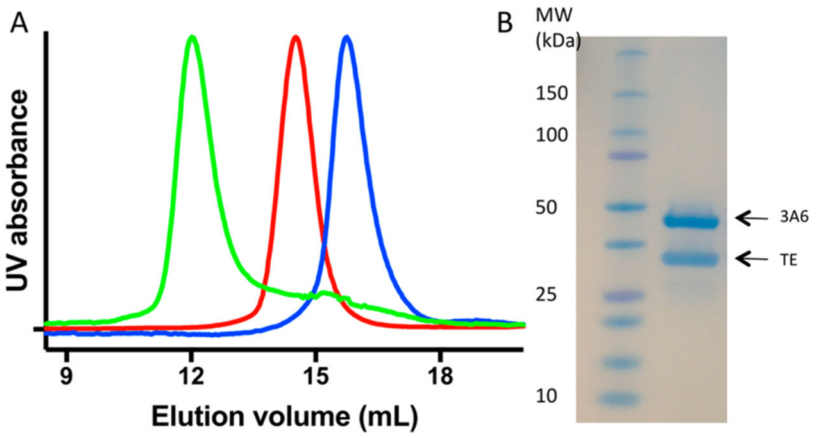

Figure 3.

Size exclusion chromatography (SEC) analysis of the 3A6–TE complex. (A) The 3A6–TE complex (green trace) showed a distinct elution profile on a Superdex 200 10/30 column compared with that of unbound 3A6 (blue) or TE (red). The narrow width of the 3A6–TE peak is consistent with its limited conformational flexibility. (B) Nonreducing SDS–PAGE analysis of the 3A6–TE peak confirmed that it contained a 1:1 stoichiometric mixture of the TE and the F_{ab}.

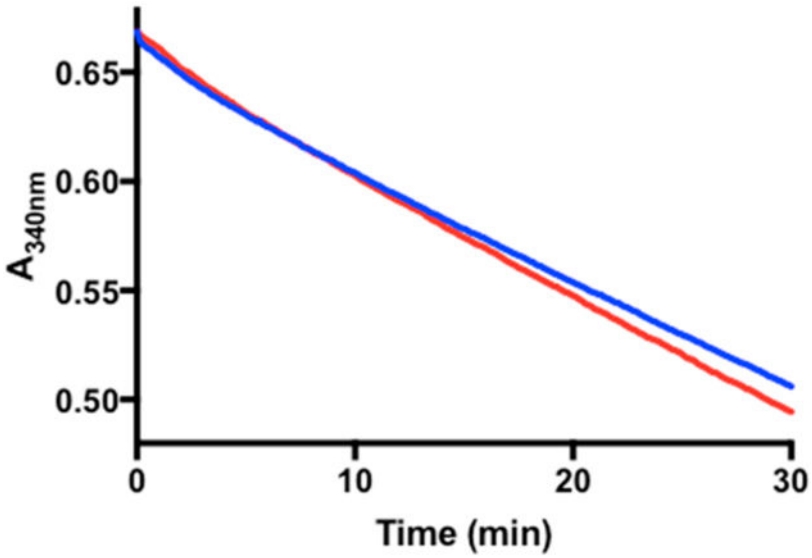

Figure 4.

3A6 does not inhibit the terminal thioesterase activity of the TE domain. The in vitro activity of the truncated trimodular derivative of DEBS (Figure 1B) was assayed in the presence of 2 μM purified LDD, 2 μM module 1, 2 μM module 2, and 2 μM M3+TE proteins. Turnover was measured by monitoring NADPH consumption by absorbance at 340 nm, as described previously.[6] The sample with excess 3A6 (red) showed a turnover rate (1.15 min^{-1}) identical to that of the reference standard (blue, 1.02 min^{-1}).

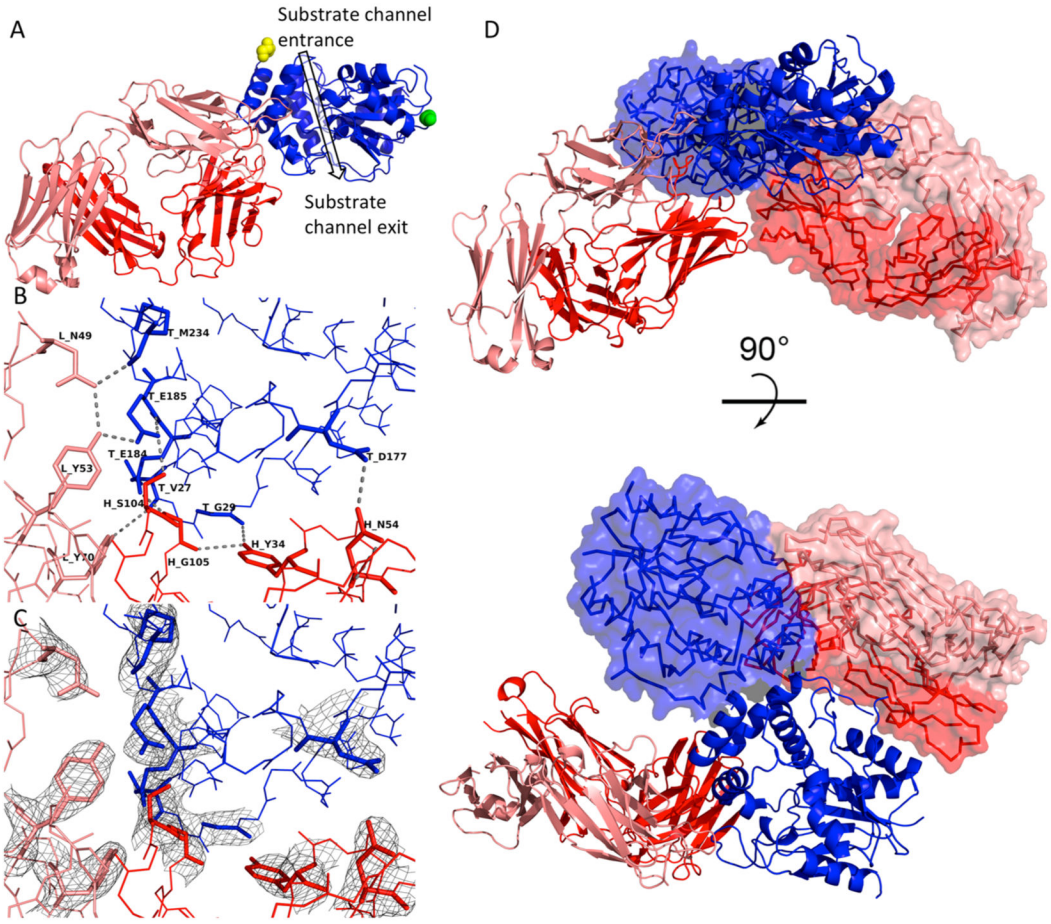

Figure 5.

Crystal structure of the 3A6–TE complex. (A) Each asymmetric structure contains one monomer (blue) of the TE homodimer and 1 equiv of 3A6 (light chain colored red, heavy chain colored dark red), confirming the 1:1 binding stoichiometry predicted by SEC analysis (Figure 3). The N- and C-termini of the TE are highlighted as yellow and green spheres, respectively, and the putative substrate tunnel is indicated by an arrow.[13](B) Residues involved in hydrogen bonding and ionic interactions at the antigen–antibody interface are shown as sticks, and the intermolecular interactions are shown as dashed lines. The coloring scheme is the same as that in panel A. The key interactions are as follows (TE = thioesterase; LC = light chain; HC = heavy chain): TE_V27 backbone carbonyl with LC_Y70 phenolic OH, TE_G29 backbone carbonyl with HC_Y34 phenolic hydroxyl, TE_D177 carboxylate with HC_N54 amide NH_2, TE_E184 carboxylate with HC_G105 backbone amide, TE_E185 carboxylate with both HC_S104 hydroxyl and LC_Y53 phenolic hydroxyl, and TE_M234 backbone carbonyl with LC N49 amide NH_2.(C) Composite omit map depicting the $2mF_o - DF_c$ electron density of F_{ab}–TE interface residues contoured at the 1.5σ level.[26] (D) Global view of the dimeric TE–3A6 complex. The dimer was generated by symmetry expansion. For the sake of clarity, one copy of the two protomers is shown as a cartoon while the other is shown as a ribbon/surface.

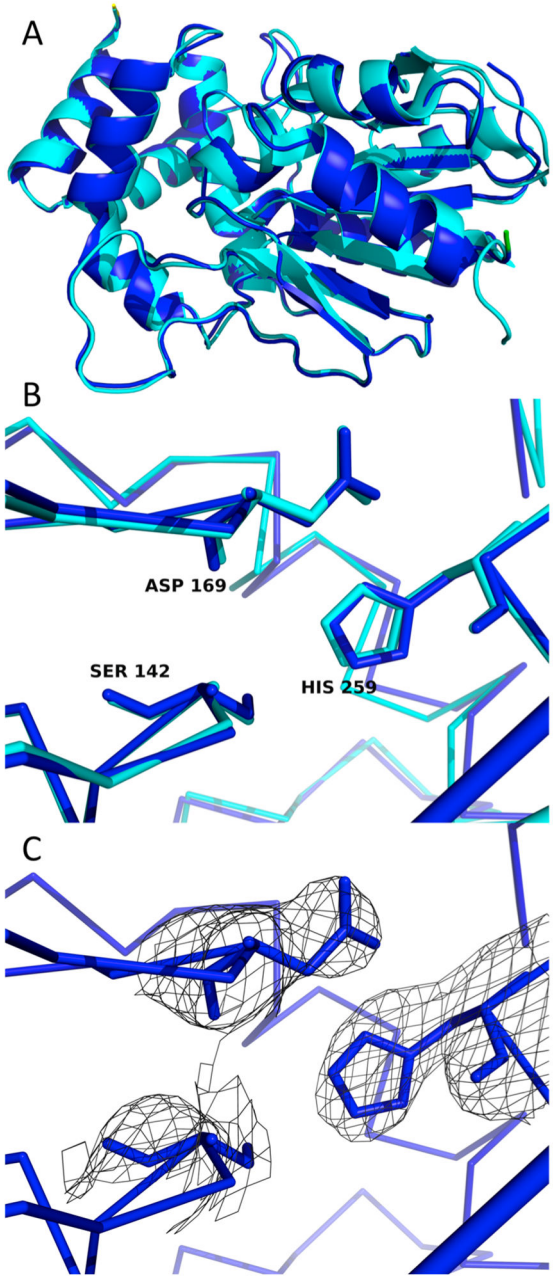

Figure 6.

3A6 binding induces minimal structural distortion in the TE structure. (A) Superimposed structures of the TE from the antibody–TE complex (blue) and the TE alone (cyan, PDB entry 5D3K[30]). The root-mean-square deviation = 0.359 Å. (B) Close-up of the TE active site, including the catalytic triad (Ser142, Asp169, and His259, shown as sticks), of the two structures. (C) Composite omit map of active site residues contoured at the 1.5σ level.[26]

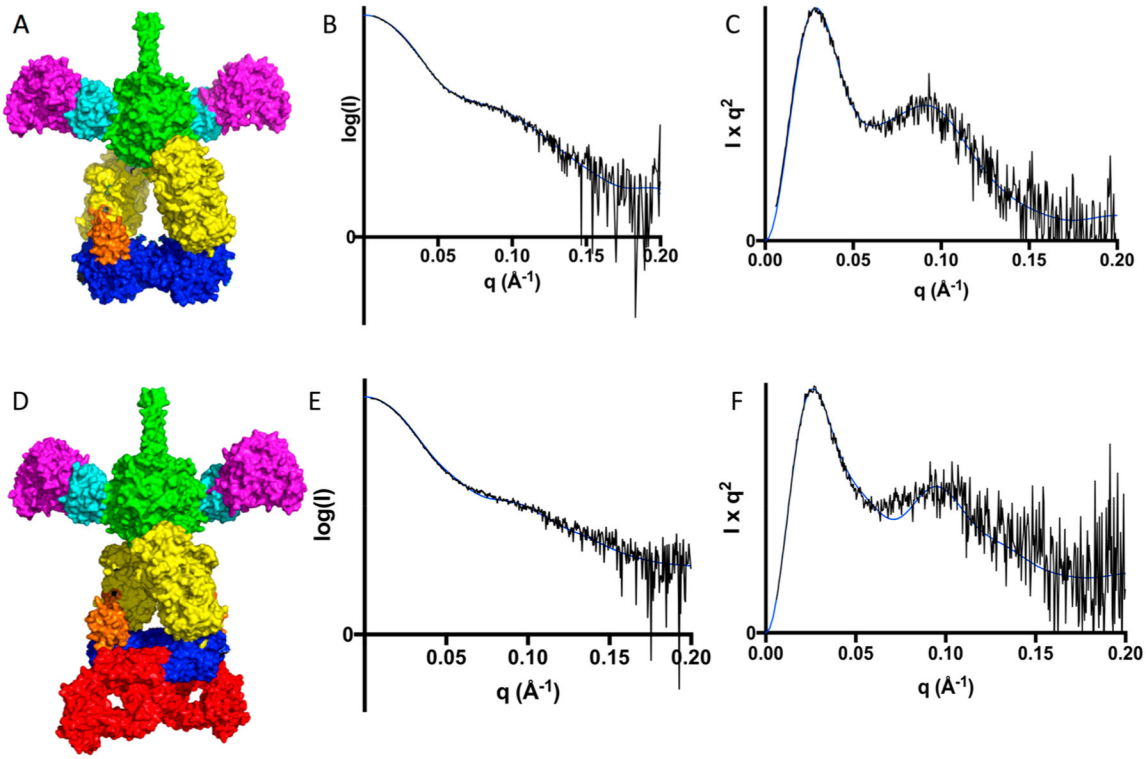

Figure 7.

Solution-phase SEC–SAXS analysis of M3+TE in the absence and presence of 3A6. (A) Model of free M3+TE derived from prior SEC–SAXS analysis of this protein.[12] Legend: F_{ab}, red; N-terminal docking domain and KS, green; KS-AT linker, cyan; AT, pink; KR, yellow; ACP, orange; TE, blue. (B) Experimentally derived scattering data [log(*I*)–*q* plot] of M3+TE showing a strong correlation (χ^2 = 0.274) to a CRYSOL simulation of the model shown in panel A. (C) Comparison of the Kratky plot of M3+TE data to the corresponding simulated curve. (D) Model of the 3A6–M3+TE complex generated by superimposing the structure shown in panel A and the X-ray crystal structure shown in Figure 5. (E) Experimentally derived scattering data [log(*I*)–*q* plot] of the 3A6–M3+TE complex showing a strong correlation (χ^2 = 0.310) to a CRYSOL simulation of the model shown in panel D. (F) Comparison of the Kratky plot of data of the 3A6–M3+TE complex to the corresponding simulated curve.

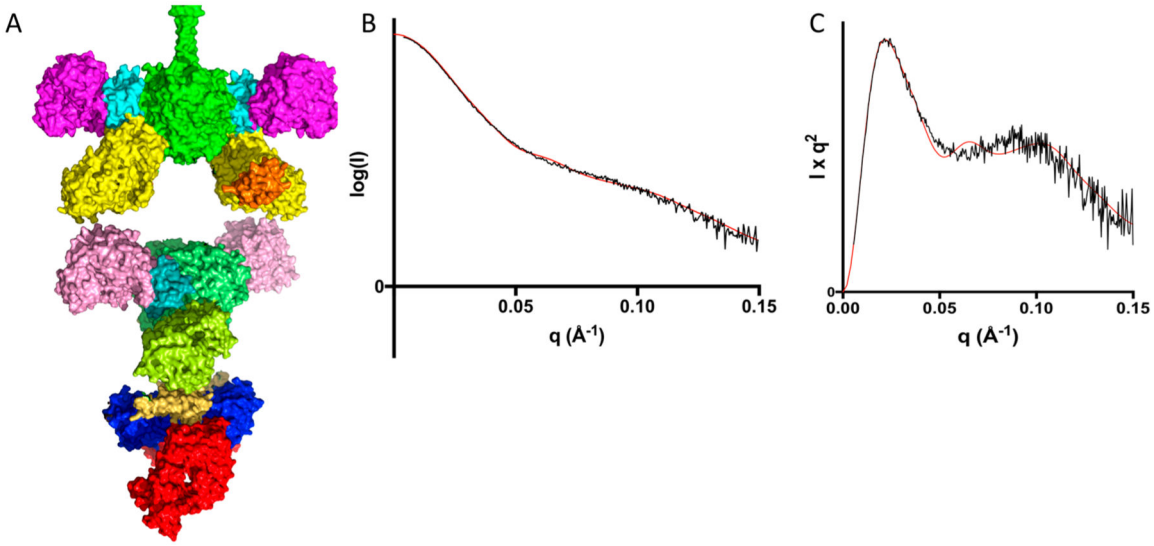

Figure 8.

Solution-phase SEC–SAXS analysis of the bimodular DEBS3 protein bound to 3A6. (A) Model of DEBS3 derived from prior SEC–SAXS analysis of this protein[12] superimposed on the crystal structure shown in Figure 5, thus generating a model of the 3A6–DEBS3 complex. The coloring scheme is identical to that in Figure 7A. (B) Experimentally derived scattering data [log(*I*)–*q* plot] from the 3A6–DEBS3 complex showing a strong correlation (χ^2 = 0.477) to a CRYSOL simulation of the model shown in panel A. (C) Comparison of the Kratky plot of the experimental data to the corresponding simulated curve.

Table 1.

Crystallographic Parameters, Data Collection Statistics, and Refinement Statistics for the Antibody 3A6–TE Complex (PDB entry 6MLK)

Crystallographic Parameters	
space group	H_{32}
unit cell dimensions	172.6 Å, 172.6 Å, 159.1 Å, 90°, 90°, 120°
Data Collection Statistics	
resolution limits (Å)	38.4–2.45
no. of observed reflections	318276
no. of unique reflections	33435
completeness (%) (overall/outer shell)	99.8/100
redundancy (overall/outer shell)	9.5/6.3
$CC_{1/2}$ (overall/outer shell)	99.8/73.8
R_{sym} [a] (%) (overall/outer shell)	9.5/93.4
I/σ (overall/outer shell)	14.2/2.0
Refinement Statistics	
resolution limits (Å)	38.4–2.45
no. of reflections/%	33432/99.8
no. of reflections used for R_{free}	1671
R_{work} [b] (%)	17.5
R_{free} [c] (%)	23.5
model contents/average B (Å^2)	
protein atoms (includes sugars)	5231/70.7
ions	1/85.6
water molecules	65/64.0
Ramachandran	
outliers/favored	0/96.1
root-mean square deviation	
bond lengths (Å)	0.009
bond angles (deg)	1.029

[a] $R_{sym} = \Sigma|I_{avg} - I_i|/\Sigma I_i$.

[b] R factor = $\Sigma|F_p - F_{pcalc}|/\Sigma F_p$, where F_p and F_{pcalc} are the observed and calculated structure factors, respectively.

[c] R_{free} is calculated with 5% of the data.

Table 2.

Summary of SAXS Data Collection and Analysis

	M3TE	M3TE–3A6	DEBS3–3A6
Data Collection Parameters			
instrument	SSRL BL4-2	SSRL BL4-2	SSRL BL4-2
type of experiment	SEC–SAXS	SEC–SAXS	SEC–SAXS
defining slit size [H(mm) × V(mm)]	0.2 × 0.2	0.2 × 0.2	0.2 × 0.2
detector distance (m)	2.5	2.5	2.5
detector	Pilatus3 × 1M	Pilatus3 × 1M	Pilatus3 × 1M
beam energy (keV)	12.4	12.4	12.4
q range (Å^{-1})	0.0046–0.40	0.0046–0.40	0.0051–0.39
exposure time per frame (s)	1	1	1
no. of frames per data set	600	600	600
temperature (K)	293	293	293
SEC Parameters			
SEC column	Superose 6 Increase PC 3.2/300	Superose 6 Increase PC 3.2/300	Superose 6 Increase PC 3.2/300
amount loaded (nmol)	0.44–2.2	0.12–1.2	0.03–0.78
HPLC flow rate (mL/min)	0.04	0.04	0.04
Structural Parameters			
I(0) from Guinier	83.826 ± 0.829	88.94 ± 1.01	216.52 ± 2.59
R_g (Å) from Guinier	61.7 ± 0.89	68.3 ± 1.13	87.9 ± 1.42
I(0) from $P(r)$	84.22	89.44	217.20
Rg (Å) from $P(r)$	62.56	69.30	89.59
D_{max} (Å) from $P(r)$	207.52	228.76	295.92
Porod volume estimate (Å^3)	835000	1150000	2050000
Software Employed			
primary data reduction	SasTool	SasTool	SasTool
data processing	PRIMUS	PRIMUS	PRIMUS
Curve Fitting Using an Atomic Model			
software employed	CRYSOL	CRYSOL	CRYSOL
q range (Å^{-1})	0.0068–0.20	0.0068–0.20	0.0055–0.15
predicted R_g (Å)	60.91	68.65	90.58
predicted D_{max} (Å)	195.3	231.3	332.3
χ^2 value	0.348	0.519	0.450
molecular weight from primary sequence (kDa)	371.4	475.8	772.6
molecular weight of atomic model (kDa)	374.9	467.7	774.5